European Congress on Computational Methods
in Applied Sciences and Engineering (ECCOMAS 2012)
J. Eberhardsteiner et.al. (eds.)
Vienna, Austria, September 10-14, 2012

COMPUTABLE BOUNDS OF LINEAR FUNCTIONAL OUTPUTS IN LINEAR VISCO-ELASTODYNAMICS

F. Verdugo[1] **and P. Díez**[1]

[1] Universitat Politècnica de Catalunya (UPC-BarcelonaTech)
Laboratori de Càlcul Numèric (LaCàN)
Jordi Girona 1-3 E-08034 Barcelona, Spain
e-mail: {francesc.verdugo,pedro.diez}@upc.edu

Keywords: computable bounds, quantity of interest, adjoint problem, goal-oriented error assessment, visco-elastodynamics

Abstract. *This work presents a new technique yielding computable bounds of quantities of interest in the framework of linear visco-elastodynamics. A novel expression for the error representation is introduced, alternative to the previous ones using the Cauchy-Schwarz inequality. The proposed formulation utilizes symmetrized forms of the error equations to derive error bounds in terms of energy error measures. The practical implementation of the method is based on constructing admissible fields for both the original problem and the adjoint problem associated with the quantity of interest. Here, the flux-free technique is considered to compute the admissible stress fields. The proposed methodology yields estimates with better quality than the ones based on the Cauchy-Schwarz inequality. In the studied examples the bound gaps obtained are approximately halved, that is the estimated intervals of confidence are reduced.*

1 INTRODUCTION

The pioneering works discussing error estimators for elliptic problems [1, 2, 3] introduced techniques assessing the energy norm of the error in Finite Element Analysis. These tools are essential to assess the reliability of numerical simulations and they are also a key ingredient for subsequent strategies providing more meaningful error measures [4, 5, 6, 7]. The latter, aiming at assessing arbitrary functional outputs of the solution describing some *quantity of interest*, are referred as *goal-oriented* error estimators.

Error estimates for elliptic (steady state) problems have reached an amazing degree of maturity, with different techniques providing excellent error estimates in an extensive collection of model problems. The error estimation tools dealing with transient problems are not so popular, especially in the case of structural dynamics. Some of the contributions on this last topic are, on the one hand, the energy error estimates presented by Aubry *et al.* [8], Li and Wiberg [9, 10] and Ladevèze *et al.* [11, 12, 13, 14] and, on the other hand, the goal-oriented estimates proposed by Schleupen and Ramm [15], Fuentes *et al.* [16] and Ladevèze and co-workers [17, 18, 19, 20].

Interest has been paid also to the error assessment tools providing bounds, that is yielding one-sided estimates (both lower bounds guaranteeing that the error is underestimated and upper bounds guaranteeing that the error is overestimated) . This topic has been addressed recently in many references, see for instance [5] where Parés *et al.* propose bounds of linear outputs for the linear elastic case. The estimates providing bounds have also been extended to transient problems, see for instance [21] where the transient convection-diffusion-reaction equation is considered. To the best knowledge of the authors, the only references discussing bounds in a quantity of interest for linear visco-elastodynamics are due to Ladevèze and co-workers [17, 18, 19, 20].

The present work aims at finding an alternative error representation improving the estimates introduced in [18]. The strategy presented in [18] is briefly revisited, using an algebraic rationale without the requirement of any thermodynamic framework. In order to simplify the developments, a linear Kelvin-Voigt constitutive relation is considered here, instead of the Maxwell model. This allows a simpler derivation, using only algebraic arguments, with no need of any mechanical consideration. The key ingredient is the computation of admissible fields for both problems. An other novelty with respect to [18] is the utilization of the flux-free technique [22] in order to build the admissible stress fields.

The remainder of this article is organized as follows. Section 2 introduces the equations of visco-elastodynamics and its numerical approximation with the Newmark method. Section 3 is devoted to obtain upper bounds of energy error measures. Section 4 discusses how to obtain bounds in quantities of interest following the error representation presented in [18]. Section 5 introduces the new error representation leading to better bounded estimates. Section 6 contains the numerical examples. The paper is closed with some concluding remarks.

2 PROBLEM STATEMENT

2.1 Governing equations

A visco-elastic body occupies the open bounded domain $\Omega \subset \mathbb{R}^d$, $d \leq 3$, with boundary $\partial\Omega$. The boundary is divided in two disjoint parts, Γ_{N} and Γ_{D} such that $\partial\Omega = \overline{\Gamma_{\mathrm{N}}} \cup \overline{\Gamma_{\mathrm{D}}}$. The time interval under consideration is $I := [0, T]$. Under the assumption of small perturbations, the evolution of displacements $\mathbf{u}(\mathbf{x}, t)$ and stresses $\boldsymbol{\sigma}(\mathbf{x}, t)$, $\mathbf{x} \in \Omega$ and $t \in I$, is described by

the visco-elastodynamic equations,

$$\rho\ddot{\mathbf{u}} - \boldsymbol{\nabla}\cdot\boldsymbol{\sigma} = \mathbf{f} \quad \text{in } \Omega\times I, \tag{1a}$$
$$\mathbf{u} = \mathbf{0} \quad \text{on } \Gamma_{\mathrm{D}}\times I, \tag{1b}$$
$$\boldsymbol{\sigma}\cdot\mathbf{n} = \mathbf{g} \quad \text{on } \Gamma_{\mathrm{N}}\times I, \tag{1c}$$
$$\mathbf{u} = \mathbf{u}_0 \quad \text{at } \Omega\times\{0\}, \tag{1d}$$
$$\dot{\mathbf{u}} = \mathbf{v}_0 \quad \text{at } \Omega\times\{0\}, \tag{1e}$$

where $\rho = \rho(\mathbf{x}) > 0$ is the mass density and an upper dot indicates partial derivation with respect to time, that is $\dot{(\bullet)} := \frac{\mathrm{d}}{\mathrm{d}t}(\bullet)$. The body force is denoted by $\mathbf{f}$, $\mathbf{g}$ is the traction acting on the Neumann boundary $\Gamma_{\mathrm{N}}\times I$ and $\mathbf{n}$ is the outward unit normal to $\partial\Omega$. Functions $\mathbf{u}_0 = \mathbf{u}_0(\mathbf{x})$ and $\mathbf{v}_0 = \mathbf{v}_0(\mathbf{x})$ are the initial conditions for displacements and velocities respectively. For the sake of simplicity and without any loss of generality, Dirichlet conditions (1b) are taken as homogeneous. The set of equations (1) is closed with the constitutive law,

$$\boldsymbol{\sigma} := \mathbf{s}(\mathbf{u}) = \mathbf{s}^{\mathrm{E}}(\mathbf{u}) + \mathbf{s}^{\nu}(\mathbf{u}), \tag{2}$$

where

$$\mathbf{s}^{\mathrm{E}}(\mathbf{w}) := \boldsymbol{\mathcal{C}} : \boldsymbol{\varepsilon}(\mathbf{w}), \tag{3a}$$
$$\mathbf{s}^{\nu}(\mathbf{w}) := \tau\boldsymbol{\mathcal{C}} : \boldsymbol{\varepsilon}(\dot{\mathbf{w}}). \tag{3b}$$

corresponding to the Kelvin-Voigt linear visco-elastic model. The parameter $\tau > 0$ is a characteristic time related with the amount of viscosity of the medium. The introduction of this parameter is fundamental in obtaining bounds. For $\tau = 0$ the bounding properties are lost. The tensor $\boldsymbol{\mathcal{C}}$ is the standard 4th-order elastic Hooke tensor. The kinematic relation (corresponding to small perturbations) $\boldsymbol{\varepsilon}(\mathbf{w}) := \frac{1}{2}(\boldsymbol{\nabla}\mathbf{w} + \boldsymbol{\nabla}^T\mathbf{w})$ is considered. The following notation is introduced for the elastic and viscous part of the stress $\boldsymbol{\sigma}$ respectively:

$$\boldsymbol{\sigma}^{\mathrm{E}} := \mathbf{s}^{\mathrm{E}}(\mathbf{u}), \tag{4a}$$
$$\boldsymbol{\sigma}^{\nu} := \mathbf{s}^{\nu}(\mathbf{u}). \tag{4b}$$

Remark 1. *The following analysis can be generalized for other more sophisticated linear Kelvin-Voigt models. These models can be introduced taking alternative expressions for* $\mathbf{s}^{\nu}$ *in equation* (3b)*.*

The subsequent analysis requires introducing a variational version of problem (1). To this end, the following spaces are introduced

$$\boldsymbol{\mathcal{W}} := \left\{ \mathbf{w} : \begin{array}{ll} \mathbf{w}(\mathbf{x},\cdot) \in [H^2(I)]^d & \forall \mathbf{x}\in\Omega \\ \mathbf{w}(\cdot,t) \in [H^1(\Omega)]^d & \forall t\in I \\ \mathbf{w} = \mathbf{0} \quad \text{at } \Gamma_{\mathrm{D}}\times I & \end{array} \right\},$$

and

$$\boldsymbol{\mathcal{U}} := \left\{ \mathbf{w}\in\boldsymbol{\mathcal{W}} : \begin{array}{ll} \mathbf{w} = \mathbf{u}_0 & \text{at } \Omega\times\{0\} \\ \dot{\mathbf{w}} = \mathbf{v}_0 & \text{at } \Omega\times\{0\} \end{array} \right\}.$$

Functions in $\boldsymbol{\mathcal{U}}$ are said to be *kinematically admissible* or *K-admissible*. They are continuous in space-time with continuous time derivative and they fulfill the initial and Dirichlet conditions. The variational version of (1) reads: find $\mathbf{u} \in \boldsymbol{\mathcal{U}}$ such that

$$B(\mathbf{u}, \mathbf{w}) = L(\mathbf{w}) \quad \forall \mathbf{w} \in \boldsymbol{\mathcal{W}}, \tag{5}$$

where

$$B(\mathbf{v}, \mathbf{w}) := \int_I (\rho \ddot{\mathbf{v}}, \dot{\mathbf{w}}) \, \mathrm{d}t + \int_I a(\mathbf{v} + \tau \dot{\mathbf{v}}, \dot{\mathbf{w}}) \, \mathrm{d}t, \tag{6a}$$

$$L(\mathbf{w}) := \int_I l(\dot{\mathbf{w}}) \, \mathrm{d}t, \tag{6b}$$

$$l(\mathbf{w}) := (\mathbf{f}, \mathbf{w}) + (\mathbf{g}, \mathbf{w})_{\Gamma_\mathrm{N}}, \tag{6c}$$

$$(\mathbf{v}, \mathbf{w}) := \int_\Omega \mathbf{v} \cdot \mathbf{w} \, \mathrm{d}\Omega, \tag{6d}$$

$$(\mathbf{v}, \mathbf{w})_{\Gamma_\mathrm{N}} := \int_{\Gamma_\mathrm{N}} \mathbf{v} \cdot \mathbf{w} \, \mathrm{d}\Gamma, \tag{6e}$$

$$a(\mathbf{v}, \mathbf{w}) := \int_\Omega \boldsymbol{\varepsilon}(\mathbf{v}) : \boldsymbol{\mathcal{C}} : \boldsymbol{\varepsilon}(\mathbf{w}) \, \mathrm{d}\Omega. \tag{6f}$$

A numerical solution of the original problem (1) may be found without using this time-space variational setting. Nevertheless, the variational formulation is useful in the following to assess the error and, in particular, in order to obtain error bounds.

3 NUMERICAL APPROXIMATION

The well known Newmark method [23] is considered for the numerical approximation of problem (1). The Newmark method is chosen because it is commonly used in practical applications and commercial codes. Note however that the present study is straightforwardly generalizable to space-time formulations, for instance those introduced by Hughes and Hulbert [24, 25].

Note that the Newmark approximation to displacements, velocities and accelerations, namely $\mathbf{u}_n^{H,\Delta t}$, $\mathbf{v}_n^{H,\Delta t}$, $\mathbf{a}_n^{H,\Delta t}$, for $n = 0, \dots N$ is not defined in the whole time interval I, but only at the time points $0 = t_0 < t_1 < \ldots < t_N = T$. However, it can be extended to the interior of the time steps using a simple linear interpolation furnishing the fields $\mathbf{u}^{H,\Delta t}$, $\mathbf{v}^{H,\Delta t}$, $\mathbf{a}^{H,\Delta t}$.

4 CONSTITUTIVE RELATION ERROR: UPPER ENERGY BOUNDS

4.1 Discretization error

Note that the numerical solution provided by the Newmark method, namely $\mathbf{u}^{H,\Delta t}$, $\mathbf{v}^{H,\Delta t}$ and $\mathbf{a}^{H,\Delta t}$, is such that the velocities are not the time derivatives of the displacements and accelerations are not the time derivatives of the velocities. Moreover, Their time dependence is not regular enough to fit in the variational setup described in equation (5), that is $\mathbf{u}^{H,\Delta t} \notin \boldsymbol{\mathcal{U}}$. A new displacement field $\hat{\mathbf{u}} \in \boldsymbol{\mathcal{U}}$ is introduced as a postprocess of the Newmark solution in order to analyze the corresponding error using the variational setup. The detailed construction of $\hat{\mathbf{u}}$ is described in section 4.5. In the remainder of the paper, the error analysis is referred to the approximate solution $\hat{\mathbf{u}}$.

The error associated with $\hat{\mathbf{u}}$, namely

$$\hat{\mathbf{e}} := \mathbf{u} - \hat{\mathbf{u}}, \tag{7}$$

lives in the space

$$\boldsymbol{\mathcal{U}}_0 := \left\{ \mathbf{w} \in \boldsymbol{\mathcal{W}} : \quad \begin{array}{ll} \mathbf{w} = \mathbf{0} & \text{at } \Omega \times \{0\} \\ \dot{\mathbf{w}} = \mathbf{0} & \text{at } \Omega \times \{0\} \end{array} \right\},$$

and fulfills the variational residual equation: find $\hat{\mathbf{e}} \in \boldsymbol{\mathcal{U}}_0$ such that

$$B(\hat{\mathbf{e}}, \mathbf{w}) = \hat{R}(\mathbf{w}) \quad \forall \mathbf{w} \in \boldsymbol{\mathcal{W}}, \tag{8}$$

where

$$\hat{R}(\mathbf{w}) := L(\mathbf{w}) - B(\hat{\mathbf{u}}, \mathbf{w}).$$

Note that the residual $\hat{R}$ does not verify the Galerkin orthogonality property because in general for arbitrary $\hat{\mathbf{u}} \in \boldsymbol{\mathcal{U}}$ and $\mathbf{w} \in \boldsymbol{\mathcal{W}}$, $B(\hat{\mathbf{u}}, \mathbf{w}) \neq L(\mathbf{w})$.

4.2 Energy measures

The first step to achieve bounds of the error $\hat{\mathbf{e}}$ in a quantity of interest is obtaining bounds of this error in a suitable energy measure. The measure to be used is associated with the following symmetric bilinear form

$$B^\nu(\mathbf{v}, \mathbf{w}) := \tau \int_I a(\mathbf{v}, \mathbf{w}) \, \mathrm{d}t. \tag{9}$$

It is useful defining equivalent versions of forms a and B^ν taking stresses as arguments:

$$\bar{a}(\boldsymbol{\tau}_1, \boldsymbol{\tau}_2) := (\boldsymbol{\tau}_1, \boldsymbol{\mathcal{C}}^{-1} : \boldsymbol{\tau}_2), \tag{10a}$$

$$\bar{B}^\nu(\boldsymbol{\tau}_1, \boldsymbol{\tau}_2) := \frac{1}{\tau} \int_I \bar{a}(\boldsymbol{\tau}_1, \boldsymbol{\tau}_2) \, \mathrm{d}t. \tag{10b}$$

The relations $a(\mathbf{v}, \mathbf{w}) = \bar{a}(\mathbf{s}^{\mathrm{E}}(\mathbf{v}), \mathbf{s}^{\mathrm{E}}(\mathbf{w}))$ and $B^\nu(\mathbf{v}, \mathbf{w}) = \bar{B}^\nu(\mathbf{s}^\nu(\mathbf{v}), \mathbf{s}^\nu(\mathbf{w}))$ hold for all $\mathbf{v}$ and $\mathbf{w}$. The bilinear forms B^ν and $\bar{B}^\nu$ lead to the energy measures:

$$|\!|\!| \mathbf{w} |\!|\!|^2 := B^\nu(\mathbf{w}, \mathbf{w}) = \tau \int_I \|\dot{\mathbf{w}}\|^2 \, \mathrm{d}t,$$

$$|\!|\!| \boldsymbol{\tau} |\!|\!|_\sigma^2 := \bar{B}^\nu(\boldsymbol{\tau}, \boldsymbol{\tau}) = \frac{1}{\tau} \int_I \|\boldsymbol{\tau}\|_\sigma^2 \, \mathrm{d}t,$$

where $\|\mathbf{w}\|^2 := a(\mathbf{w}, \mathbf{w})$ and $\|\boldsymbol{\tau}\|_\sigma^2 := \bar{a}(\boldsymbol{\tau}, \boldsymbol{\tau})$. Note that the notation introduced above is such that norms with subscript "σ" and bilinear forms with upper bar take stresses as arguments.

4.3 Admissible fields

The construction of an admissible pair $(\hat{\boldsymbol{\sigma}}, \hat{\mathbf{u}}) \in \boldsymbol{\mathcal{S}}(\hat{\mathbf{u}}) \times \boldsymbol{\mathcal{U}}$ is the key ingredient in order to obtain upper bounds of the energy of $\hat{\mathbf{e}}$. The space of admissible stresses $\boldsymbol{\mathcal{S}}(\hat{\mathbf{u}})$ is defined for a given $\hat{\mathbf{u}} \in \boldsymbol{\mathcal{U}}$ as follows

$$\boldsymbol{\mathcal{S}}(\hat{\mathbf{u}}) := \left\{ \boldsymbol{\tau} \in \boldsymbol{\mathcal{Z}} : \int_I (\boldsymbol{\tau}, \boldsymbol{\varepsilon}(\dot{\mathbf{w}})) \, \mathrm{d}t = L(\mathbf{w}) - \int_I (\rho \ddot{\hat{\mathbf{u}}}, \dot{\mathbf{w}}) \, \mathrm{d}t \quad \forall \mathbf{w} \in \boldsymbol{\mathcal{W}} \right\}, \tag{12}$$

where

$$\boldsymbol{\mathcal{Z}} := \left\{ \boldsymbol{\tau} : \quad [\boldsymbol{\tau}]_{ij} \in L^2(\Omega \times I) \quad i, j \leq d \right\},$$

and for $\boldsymbol{\tau}, \boldsymbol{\varepsilon} \in \boldsymbol{\mathcal{Z}}$

$$(\boldsymbol{\tau}, \boldsymbol{\varepsilon}) := \int_\Omega \boldsymbol{\tau} : \boldsymbol{\varepsilon} \, \mathrm{d}\Omega.$$

The space $\boldsymbol{\mathcal{S}}(\hat{\mathbf{u}})$ contains the *dynamically admissible* or *D-admissible* stresses. These stress tensors are in dynamic equilibrium with respect the external loads and with the inertia forces related to the admissible acceleration $\ddot{\hat{\mathbf{u}}}$. They can be discontinuous between mesh elements but the vector $\hat{\boldsymbol{\sigma}} \cdot \mathbf{n}$ has to be continuous across element edges. Note that the definition of $\boldsymbol{\mathcal{S}}(\hat{\mathbf{u}})$ requires the previous selection of a field $\hat{\mathbf{u}} \in \boldsymbol{\mathcal{U}}$. This is a particularity of the dynamic case. A method to build a D-admissible field $\hat{\boldsymbol{\sigma}}$ from the numerical solution $\hat{\mathbf{u}}$ is shown in section 4.6.

In the following, it is usefull to introduce the notations

$$\hat{\boldsymbol{\sigma}}^{\mathrm{E}} := \mathbf{s}^{\mathrm{E}}(\hat{\mathbf{u}}), \tag{13a}$$

$$\hat{\boldsymbol{\sigma}}^{\nu} := \hat{\boldsymbol{\sigma}} - \hat{\boldsymbol{\sigma}}^{\mathrm{E}}, \tag{13b}$$

which are a decomposition of the admissible stress $\hat{\boldsymbol{\sigma}}$ into elastic and viscous parts, i.e. $\hat{\boldsymbol{\sigma}} = \hat{\boldsymbol{\sigma}}^{\mathrm{E}} + \hat{\boldsymbol{\sigma}}^{\nu}$.

4.4 Global error representation and computable error bounds

The admissible pair $(\hat{\boldsymbol{\sigma}}, \hat{\mathbf{u}}) \in \boldsymbol{\mathcal{S}}(\hat{\mathbf{u}}) \times \boldsymbol{\mathcal{U}}$ defines the following error in stresses

$$\hat{\boldsymbol{\sigma}}^{\mathrm{e}} := \hat{\boldsymbol{\sigma}} - \mathbf{s}(\hat{\mathbf{u}}). \tag{14}$$

This error corresponds to the non verification of the constitutive relation (2) associated with the admissible pair. The value $\|\hat{\boldsymbol{\sigma}}^{\mathrm{e}}\|_\sigma$ is the so called *constitutive relation error* (following the terminology by Ladevèze and co-workers) and it is computable once the fields $\hat{\boldsymbol{\sigma}}$ and $\hat{\mathbf{u}}$ available. Note that, $\|\hat{\boldsymbol{\sigma}}^{\mathrm{e}}\|_\sigma = 0$ if and only if $\hat{\boldsymbol{\sigma}} = \boldsymbol{\sigma}$ and $\hat{\mathbf{u}} = \mathbf{u}$. Consequently, $\|\hat{\boldsymbol{\sigma}}^{\mathrm{e}}\|_\sigma$ is adopted as a pertinent error measure. Moreover, the value $\|\hat{\boldsymbol{\sigma}}^{\mathrm{e}}\|_\sigma$ is also meaningful because it is related with the unknown error $\hat{\mathbf{e}}$.

Theorem 1. *Given an admissible pair* $(\hat{\boldsymbol{\sigma}}, \hat{\mathbf{u}}) \in \boldsymbol{\mathcal{S}}(\hat{\mathbf{u}}) \times \boldsymbol{\mathcal{U}}$*, the errors defined in equations* (14) *and* (7)*,* $\hat{\boldsymbol{\sigma}}^{\mathrm{e}}$ *and* $\hat{\mathbf{e}}$*, fulfill*

$$\|\hat{\boldsymbol{\sigma}}^{\mathrm{e}}\|_\sigma^2 = |\dot{\hat{\mathbf{e}}}|_{t=T}^2 + \|\hat{\mathbf{e}}\|_{t=T}^2 + |||\hat{\mathbf{e}}|||^2 + \|\boldsymbol{\sigma}^{\nu} - \hat{\boldsymbol{\sigma}}^{\nu}\|_\sigma^2. \tag{15}$$

being $\boldsymbol{\sigma}^{\nu}$ *and* $\hat{\boldsymbol{\sigma}}^{\nu}$ *defined in* (4b) *and* (13b)*.*

Theorem 1 furnishes the relation $\|\hat{\boldsymbol{\sigma}}^{\mathrm{e}}\|_\sigma^2 \geq |\dot{\hat{\mathbf{e}}}|_{t=T}^2 + \|\hat{\mathbf{e}}\|_{t=T}^2 + |||\hat{\mathbf{e}}|||^2$ and, in particular, the following upper bound

$$\|\hat{\boldsymbol{\sigma}}^{\mathrm{e}}\|_\sigma \geq |||\hat{\mathbf{e}}|||. \tag{16}$$

Expression (16) is particularly important because it is used to bound the quantity of interest.

4.5 Construction of K-admissible fields

The firs step to build an admissible pair $(\hat{\boldsymbol{\sigma}}, \hat{\mathbf{u}}) \in \boldsymbol{\mathcal{S}}(\hat{\mathbf{u}}) \times \boldsymbol{\mathcal{U}}$ is to define the K-admissible field $\hat{\mathbf{u}} \in \boldsymbol{\mathcal{U}}$. The method of the linear accelerations [26, Ch. 7] is considered in the present case. This method is preferred because it simplifies the subsequent construction of the D-admissible field.

The basic idea is to take the admissible acceleration equal to $\mathbf{a}^{H,\Delta t}$ and then integrate in time to obtain the admissible velocity and the admissible displacement:

$$\ddot{\hat{\mathbf{u}}}(\mathbf{x},t) := \mathbf{a}^{H,\Delta t}(\mathbf{x},t), \tag{17a}$$

$$\dot{\hat{\mathbf{u}}}(\mathbf{x},t) := \int_0^t \ddot{\mathbf{u}}^{H,\Delta t}(\mathbf{x},\xi)\,\mathrm{d}\xi + \mathbf{v}_0^{H,\Delta t}(\mathbf{x}), \tag{17b}$$

$$\hat{\mathbf{u}}(\mathbf{x},t) := \int_0^t \dot{\hat{\mathbf{u}}}^{H,\Delta t}(\mathbf{x},\xi)\,\mathrm{d}\xi + \mathbf{u}_0^{H,\Delta t}(\mathbf{x}). \tag{17c}$$

4.6 Construction of D-admissible fields

Once the field $\hat{\mathbf{u}} \in \boldsymbol{\mathcal{U}}$ is available, the D-admissible field is built such that $\hat{\boldsymbol{\sigma}} \in \boldsymbol{\mathcal{S}}(\hat{\mathbf{u}})$. The construction of $\hat{\boldsymbol{\sigma}}$ is more involved than the one for $\hat{\mathbf{u}}$. The reason is that the admissible stress has to be equilibrated in a dynamic sense. Under certain circumstances, this dynamic equilibration is reduced to static equilibration at each time $t \in \mathcal{T}$. This allows using the standard equilibration techniques for the static problem that are well studied in the literature [26, 27, 28, 22].

The methods allowing to compute a D-admissible stress field with an affordable computational cost require using domain decomposition. The two main approaches for domain decomposition are the hybrid-flux [26] and the flux-free methodologies [22], using respectively as local subdomains the elements and patches of elements centered in one node (stars). Other approaches furnish D-admissible fields solving global dual problems (having stresses as unknowns) on the original finite element mesh, see for instance [29, 30]. Here, the asymptotic flux-free approach is selected.

5 BOUNDS OF LINEAR FUNCTIONAL OUTPUTS

5.1 Quantity of interest

The present study aims at obtaining bounds for some given quantity of interest of the solution, denoted by $L^{\mathcal{O}}(\mathbf{u})$, being $L^{\mathcal{O}}$ a linear form such that

$$\begin{aligned} L^{\mathcal{O}} : \boldsymbol{\mathcal{U}} &\longrightarrow \mathbb{R} \\ \mathbf{w} &\longmapsto L^{\mathcal{O}}(\mathbf{w}). \end{aligned}$$

The structure of $L^{\mathcal{O}}$ is restricted to be as follows:

$$\begin{aligned} L^{\mathcal{O}}(\mathbf{w}) := & \int_I (\mathbf{f}^{\mathcal{O}}, \dot{\mathbf{w}})\,\mathrm{d}t && \text{(average of velocities in } \Omega\times I) \\ & + \int_I (\mathbf{g}^{\mathcal{O}}, \dot{\mathbf{w}})_{\Gamma_{\mathrm{N}}}\,\mathrm{d}t && \text{(average of velocities on } \Gamma_{\mathrm{N}}\times I) \\ & + (\rho\mathbf{v}^{\mathcal{O}}, \dot{\mathbf{w}}(T)) && \text{(average of velocities at } \Omega\times\{T\}) \\ & + a(\mathbf{u}^{\mathcal{O}}, \mathbf{w}(T)) && \text{(average of strains at } \Omega\times\{T\}), \end{aligned} \tag{18}$$

where $\mathbf{f}^{\mathcal{O}}$, $\mathbf{g}^{\mathcal{O}}$, $\mathbf{v}^{\mathcal{O}}$ and $\mathbf{u}^{\mathcal{O}}$ are the data characterizing the quantity of interest. The interpretation of each term of the previous equation is indicated inline, being $\mathbf{w}$ a displacement. This functional is rewritten in a more compact form:

$$L^{\mathcal{O}}(\mathbf{w}) = L^{\mathrm{d}}(\mathbf{w}) + (\rho\mathbf{v}^{\mathcal{O}}, \dot{\mathbf{w}}(T)) + a(\mathbf{u}^{\mathcal{O}}, \mathbf{w}(T)), \tag{19}$$

where

$$L^{\mathrm{d}}(\mathbf{w}) := \int_I l^{\mathrm{d}}(\dot{\mathbf{w}})\,\mathrm{d}t,$$
$$l^{\mathrm{d}}(\mathbf{v}) := (\mathbf{f}^{\mathcal{O}}, \mathbf{w}) + (\mathbf{g}^{\mathcal{O}}, \mathbf{w})_{\Gamma_{\mathrm{N}}}.$$

5.2 Adjoint problem

The *adjoint* or *dual* problem of equations (1) associated with the quantity of interest given in (18) consists in finding $\mathbf{u}^{\mathrm{d}}$ such that

$$\rho\ddot{\mathbf{u}}^{\mathrm{d}} - \boldsymbol{\nabla}\cdot\boldsymbol{\sigma}^{\mathrm{d}} = \mathbf{f}^{\mathcal{O}} \quad \text{in } \Omega\times I, \tag{21a}$$
$$\mathbf{u}^{\mathrm{d}} = \mathbf{0} \quad \text{on } \Gamma_{\mathrm{D}}\times I, \tag{21b}$$
$$\boldsymbol{\sigma}^{\mathrm{d}}\cdot\mathbf{n} = \mathbf{g}^{\mathcal{O}} \quad \text{on } \Gamma_{\mathrm{N}}\times I, \tag{21c}$$
$$\mathbf{u}^{\mathrm{d}} = -\mathbf{u}^{\mathcal{O}} \quad \text{at } \Omega\times\{T\}, \tag{21d}$$
$$\dot{\mathbf{u}}^{\mathrm{d}} = -\mathbf{v}^{\mathcal{O}} \quad \text{at } \Omega\times\{T\}, \tag{21e}$$

with the constitutive law

$$\boldsymbol{\sigma}^{\mathrm{d}} := \boldsymbol{\mathcal{C}} : \boldsymbol{\varepsilon}(\mathbf{u}^{\mathrm{d}} - \tau\dot{\mathbf{u}}^{\mathrm{d}}). \tag{22}$$

The external loads and final conditions of the adjoint problem are determined by the definition of quantity of interest in equation (18). The adjoint problem has not the same form as the original one because it has final conditions instead of initial ones and negative damping.

Remark 2. *The adjoint problem* (21) *has the same form as the original* (1) *if integrated backwards in time. That is to say, introducing the change of variables* $t^\star := T - t$.

A variational setting for the adjoint problem (21) is required in the following. To this end, the adjoint trial space is defined as

$$\boldsymbol{\mathcal{U}}^{\mathrm{d}} := \left\{ \mathbf{w}\in\boldsymbol{\mathcal{W}} : \begin{array}{ll} \mathbf{w} = -\mathbf{u}^{\mathcal{O}} & \text{at } \Omega\times\{T\}, \\ \dot{\mathbf{w}} = -\mathbf{v}^{\mathcal{O}} & \text{at } \Omega\times\{T\} \end{array} \right\}.$$

The set $\boldsymbol{\mathcal{U}}^{\mathrm{d}}$ contains the *adjoint kinematically admissible* or *adjoint K-admissible* displacements. These functions have the same regularity constrains and boundary conditions as the ones in $\boldsymbol{\mathcal{U}}$ and the final conditions of the adjoint problem (21).

With this notation, the weak form of the adjoint problem (21) reads: find $\mathbf{u}^{\mathrm{d}}\in\boldsymbol{\mathcal{U}}^{\mathrm{d}}$ such that

$$B^{\mathrm{d}}(\mathbf{u}^{\mathrm{d}}, \mathbf{w}) = L^{\mathrm{d}}(\mathbf{w}) \quad \forall\mathbf{w}\in\boldsymbol{\mathcal{W}}, \tag{23}$$

where for $\mathbf{v}, \mathbf{w}\in\boldsymbol{\mathcal{W}}$

$$B^{\mathrm{d}}(\mathbf{v}, \mathbf{w}) := \int_I (\rho\ddot{\mathbf{v}}, \dot{\mathbf{w}})\,\mathrm{d}t + \int_I a(\mathbf{v} - \tau\dot{\mathbf{v}}, \dot{\mathbf{w}})\,\mathrm{d}t.$$

5.3 Error representation in the quantity of interest

Bounds of the quantity of interest $L^{\mathcal{O}}(\mathbf{u})$ are obtained combining admissible pairs for both the original and the adjoint problem, $(\hat{\boldsymbol{\sigma}}, \hat{\mathbf{u}})$ and $(\hat{\boldsymbol{\sigma}}^{\mathrm{d}}, \hat{\mathbf{u}}^{\mathrm{d}})$. These admissible pairs allow to express the error in the quantity of interest $L^{\mathcal{O}}(\hat{\mathbf{e}})$ in terms of energy products, see theorem 2

below. Moreover, bounds for the quantity of interest are obtained from energy estimates, using equation (16) or similar variations.

The admissible pair for the the adjoint problem (21) is obtained such that $(\hat{\boldsymbol{\sigma}}^{\mathrm{d}}, \hat{\mathbf{u}}^{\mathrm{d}}) \in \boldsymbol{\mathcal{S}}(\hat{\mathbf{u}}^{\mathrm{d}}) \times \boldsymbol{\mathcal{U}}^{\mathrm{d}}$. The space of *adjoint dynamically admissible* or *adjoint D-admissible* fields is defined for a given $\hat{\mathbf{u}}^{\mathrm{d}} \in \boldsymbol{\mathcal{U}}^{\mathrm{d}}$ as follows

$$\boldsymbol{\mathcal{S}}^{\mathrm{d}}(\hat{\mathbf{u}}^{\mathrm{d}}) := \left\{ \boldsymbol{\tau} \in \boldsymbol{\mathcal{Z}} : \quad \int_I (\boldsymbol{\tau}, \boldsymbol{\varepsilon}(\dot{\mathbf{w}}))\, \mathrm{d}t = L^{\mathrm{d}}(\mathbf{w}) - \int_I (\rho \ddot{\hat{\mathbf{u}}}^{\mathrm{d}}, \dot{\mathbf{w}})\, \mathrm{d}t \quad \forall \mathbf{w} \in \boldsymbol{\mathcal{W}} \right\}.$$

The space $\boldsymbol{\mathcal{S}}^{\mathrm{d}}(\hat{\mathbf{u}}^{\mathrm{d}})$ contains stress tensors in dynamic equilibrium respect to the loads of the adjoint problem and the inertia related to the acceleration $\ddot{\hat{\mathbf{u}}}^{\mathrm{d}}$.

The admissible pair $(\hat{\boldsymbol{\sigma}}^{\mathrm{d}}, \hat{\mathbf{u}}^{\mathrm{d}}) \in \boldsymbol{\mathcal{S}}(\hat{\mathbf{u}}^{\mathrm{d}}) \times \boldsymbol{\mathcal{U}}^{\mathrm{d}}$ determines the error in stresses for the adjoint problem:

$$\hat{\boldsymbol{\sigma}}^{\mathrm{d,e}} := \hat{\boldsymbol{\sigma}}^{\mathrm{d}} - \mathbf{s}^{\mathrm{E}}(\hat{\mathbf{u}}^{\mathrm{d}}) + \mathbf{s}^{\nu}(\hat{\mathbf{u}}^{\mathrm{d}}),$$

which corresponds to the non verification of the constitutive relation of the adjoint problem (22). The constitutive relation error of the adjoint problem is the value $\|\hat{\boldsymbol{\sigma}}^{\mathrm{d,e}}\|_{\sigma}$.

The errors $\hat{\boldsymbol{\sigma}}^{\mathrm{e}}$ and $\hat{\boldsymbol{\sigma}}^{\mathrm{d,e}}$ are seen as the solutions of the residual error equations

$$\bar{B}^{\nu}(\hat{\boldsymbol{\sigma}}^{\mathrm{e}}, \mathbf{s}^{\nu}(\mathbf{w})) = \hat{R}(\mathbf{w}) \quad \forall \mathbf{w} \in \boldsymbol{\mathcal{W}}, \tag{24a}$$

$$\bar{B}^{\nu}(\hat{\boldsymbol{\sigma}}^{\mathrm{d,e}}, \mathbf{s}^{\nu}(\mathbf{w})) = \hat{R}^{\mathrm{d}}(\mathbf{w}) \quad \forall \mathbf{w} \in \boldsymbol{\mathcal{W}}, \tag{24b}$$

where the residual for the adjoint problem is defined by

$$\hat{R}^{\mathrm{d}}(\mathbf{w}) := L^{\mathrm{d}}(\mathbf{w}) - B^{\mathrm{d}}(\hat{\mathbf{u}}^{\mathrm{d}}, \mathbf{w}).$$

The previous relations are easily derived from the definition of D-admissibility. For instance, equation (24a) follows from the property included in the definition of $\boldsymbol{\mathcal{S}}(\hat{\mathbf{u}})$ in equation (12) by simply subtracting $\int_I a(\hat{\mathbf{u}} + \tau\dot{\hat{\mathbf{u}}}, \dot{\mathbf{w}})\, \mathrm{d}t$ at each hand side. The proof for (24b) is analogous.

Theorem 2. *If $(\hat{\boldsymbol{\sigma}}, \hat{\mathbf{u}}) \in \boldsymbol{\mathcal{S}}(\hat{\mathbf{u}}) \times \boldsymbol{\mathcal{U}}$ and $(\hat{\boldsymbol{\sigma}}^{d}, \hat{\mathbf{u}}^{d}) \in \boldsymbol{\mathcal{S}}^{d}(\hat{\mathbf{u}}^{d}) \times \boldsymbol{\mathcal{U}}^{d}$ are two admissible pairs for the original and adjoint problems, then the following error representation holds*

$$L^{\mathcal{O}}(\hat{\mathbf{e}}) + \hat{\alpha} = \hat{R}^{\mathrm{d}}(\hat{\mathbf{e}}), \tag{25}$$

or alternatively

$$L^{\mathcal{O}}(\hat{\mathbf{e}}) + \hat{\alpha} = \bar{B}^{\nu}(\hat{\boldsymbol{\sigma}}^{\mathrm{d,e}}, \mathbf{s}^{\nu}(\hat{\mathbf{e}})), \tag{26}$$

where $\hat{\alpha}$ is the following correcting term

$$\hat{\alpha} := \hat{R}(\hat{\mathbf{u}}^{\mathrm{d}}) = \bar{B}^{\nu}(\hat{\boldsymbol{\sigma}}^{\mathrm{e}}, \mathbf{s}^{\nu}(\hat{\mathbf{u}}^{\mathrm{d}})).$$

As previously said, this result relates $L^{\mathcal{O}}(\hat{\mathbf{e}})$ with the energy-like quantities $\hat{R}^{\mathrm{d}}(\hat{\mathbf{e}})$ and $\bar{B}^{\nu}(\hat{\boldsymbol{\sigma}}^{\mathrm{d,e}}, \mathbf{s}^{\nu}(\hat{\mathbf{e}}))$. Note that $\hat{\alpha}$ accounts for the lack of Galerkin orthogonality of residual $\hat{R}$ and it is computable once the admissible fields are available.

5.4 Bounds based on the Cauchy-Schwarz inequality

Bounds based on the Cauchy-Schwarz inequality are already introduced for visco-elastodynamics in reference [18]. These bounds are derived from the error representation in equation (26) along with the Cauchy-Schwarz inequality:

$$|L^{\mathcal{O}}(\hat{\mathbf{e}}) + \hat{\alpha}| \leq \|\hat{\boldsymbol{\sigma}}^{\mathrm{d,e}}\|_{\sigma} \|\mathbf{s}^{\nu}(\hat{\mathbf{e}})\|_{\sigma} = \|\hat{\boldsymbol{\sigma}}^{\mathrm{d,e}}\|_{\sigma} \|\hat{\mathbf{e}}\|. \tag{27}$$

Note that the last factor in the latter expression is not computable because involves the unknown error $\hat{\mathbf{e}}$. An upper bound estimate for this factor is the error in the constitutive relation of the original problem, see equation (16). Introducing this estimate in the previous equation a computable bound for the error in the quantity of interest is readily recovered:

$$|L^{\mathcal{O}}(\hat{\mathbf{e}}) + \hat{\alpha}| \leq \|\hat{\boldsymbol{\sigma}}^{\mathrm{d,e}}\|_{\sigma} \|\hat{\boldsymbol{\sigma}}^{\mathrm{e}}\|_{\sigma}.$$

The quantities defined as

$$\begin{aligned} \zeta_{\mathrm{U}}^{\mathrm{C\text{–}S}} &:= L^{\mathcal{O}}(\hat{\mathbf{u}}) + \|\hat{\boldsymbol{\sigma}}^{\mathrm{d,e}}\|_{\sigma} \|\hat{\boldsymbol{\sigma}}^{\mathrm{e}}\|_{\sigma} - \hat{\alpha}, \\ \zeta_{\mathrm{L}}^{\mathrm{C\text{–}S}} &:= L^{\mathcal{O}}(\hat{\mathbf{u}}) - \|\hat{\boldsymbol{\sigma}}^{\mathrm{d,e}}\|_{\sigma} \|\hat{\boldsymbol{\sigma}}^{\mathrm{e}}\|_{\sigma} - \hat{\alpha}, \end{aligned}$$

are indeed upper and lower bounds of $L^{\mathcal{O}}(\mathbf{u})$, that is

$$\zeta_{\mathrm{L}}^{\mathrm{C\text{–}S}} \leq L^{\mathcal{O}}(\mathbf{u}) \leq \zeta_{\mathrm{U}}^{\mathrm{C\text{–}S}}. \tag{29}$$

6 Alternative error bounds

6.1 Alternative error representation and (non-computable) bounds

Alternative error bounds are often used in the literature to improve the poor quality of the bounds based on the Cauchy-Schwarz inequality. For instance, the parallelogram rule is applied in works [7, 31, 22] in the context of linear elasticity. Similar strategies based on algebraic identities are also applied to problems with non-symmetric bilinear forms as the case of the steady and transient convection-diffusion-reaction equations, see reference [21]. However, to the best knowledge of the authors, these kind of approaches have not been used in the framework of linear visco-elastodynamics.

In the following, an alternative error representation is used to derive error bounds for quantities of interest in the context of visco-elastodynamics. The derivation of the basic rationale requires introducing symmetrized equations for the original and adjoint errors. Note, however, that the actual implementation of these strategies does not require solving the auxiliary symmetrized problems because the upper bound estimates are computed using only the admissible fields introduced above. These ideas are similar to those used in [21].

Consider the following symmetrized error equations: find $\hat{\mathbf{e}}^{\nu} \in \boldsymbol{\mathcal{U}}_0$ and $\hat{\mathbf{e}}^{\mathrm{d},\nu} \in \boldsymbol{\mathcal{U}}_0^{\mathrm{d}}$ such that

$$B^{\nu}(\hat{\mathbf{e}}^{\nu}, \mathbf{w}) = \hat{R}(\mathbf{w}) \quad \forall \mathbf{w} \in \boldsymbol{\mathcal{W}}, \tag{30a}$$

$$B^{\nu}(\hat{\mathbf{e}}^{\mathrm{d},\nu}, \mathbf{w}) = \hat{R}^{\mathrm{d}}(\mathbf{w}) \quad \forall \mathbf{w} \in \boldsymbol{\mathcal{W}}, \tag{30b}$$

where

$$B^{\nu}(\mathbf{v}, \mathbf{w}) := \tau \int_I a(\mathbf{v}, \mathbf{w}) \, \mathrm{d}t,$$

and

$$\boldsymbol{\mathcal{U}}_0^{\mathrm{d}} := \left\{ \mathbf{w} \in \boldsymbol{\mathcal{W}} : \quad \begin{array}{ll} \mathbf{w} = \mathbf{0} & \text{at } \Omega \times \{T\} \\ \dot{\mathbf{w}} = \mathbf{0} & \text{at } \Omega \times \{T\} \end{array} \right\}.$$

Equations (30) resemble the residual equation (8) for the error $\hat{\mathbf{e}}$. Note that the difference is that the bilinear form B is replaced by the symmetric one B^ν.

Theorem 3. *If* $\hat{\mathbf{e}}^\nu$ *and* $\hat{\mathbf{e}}^{\mathrm{d},\nu}$ *are solution of equations* (30a) *and* (30b) *then, for any* $\kappa \in \mathbb{R}$, $\kappa \neq 0$,

$$-\frac{1}{4}\|\kappa\hat{\mathbf{e}}^\nu - \frac{1}{\kappa}\hat{\mathbf{e}}^{\mathrm{d},\nu}\|^2 \leq L^{\mathcal{O}}(\hat{\mathbf{e}}) + \hat{\alpha} \leq \frac{1}{4}\|\kappa\hat{\mathbf{e}}^\nu + \frac{1}{\kappa}\hat{\mathbf{e}}^{\mathrm{d},\nu}\|^2. \tag{31}$$

Equation (31) allows bounding $L^{\mathcal{O}}(\hat{\mathbf{e}})$ by computing $\|\mathbf{z}^\pm\|^2$, where $\mathbf{z}^\pm := \kappa\hat{\mathbf{e}}^\nu \pm \frac{1}{\kappa}\hat{\mathbf{e}}^{\mathrm{d},\nu}$. These two functions are solutions of

$$B^\nu(\mathbf{z}^\pm, \mathbf{w}) = \hat{R}^\pm(\mathbf{w}) \quad \forall \mathbf{w} \in \boldsymbol{\mathcal{W}}, \tag{32}$$

where

$$\hat{R}^\pm(\mathbf{w}) := \kappa\hat{R}(\mathbf{w}) \pm \frac{1}{\kappa}\hat{R}^{\mathrm{d}}(\mathbf{w}).$$

Functions $\mathbf{z}^\pm$ are solutions of the infinite dimensional problems (32). Therefore, the error bounds proposed in (31), corresponding to the values of $\|\mathbf{z}^\pm\|^2$, are not computable. In the following, computable bounds are obtained from an auxiliary field $\boldsymbol{\sigma}_{\mathbf{z}^\pm}$, in the same fashion as the energy-like bounds described in section 4.

6.2 Computable error bounds

As shown in section 4 the standard approach to obtain a computable error bound is to find a D-admissible stress. The admissible stress associated with $\mathbf{z}^\pm$ is denoted by $\boldsymbol{\sigma}_{\mathbf{z}^\pm}$ which fulfills the stress-version of equation (32), i.e.

$$\bar{B}^\nu(\boldsymbol{\sigma}_{\mathbf{z}^\pm}, \mathbf{s}^\nu(\mathbf{w})) = \hat{R}^\pm(\mathbf{w}) \quad \forall \mathbf{w} \in \boldsymbol{\mathcal{W}}. \tag{33}$$

Comparing equation (33) and the residual representation of equations (24), one concludes that the following linear combination of $\hat{\boldsymbol{\sigma}}^{\mathrm{e}}$ and $\hat{\boldsymbol{\sigma}}^{\mathrm{d,e}}$

$$\boldsymbol{\sigma}_{\mathbf{z}^\pm} := \kappa\hat{\boldsymbol{\sigma}}^{\mathrm{e}} \pm \frac{1}{\kappa}\hat{\boldsymbol{\sigma}}^{\mathrm{d,e}}, \tag{34}$$

is solution of (33). The value $\|\boldsymbol{\sigma}_{\mathbf{z}^\pm}\|_\sigma$ is indeed an upper bound of $\|\mathbf{z}^\pm\|$. Thus, using expression (34) for $\boldsymbol{\sigma}_{\mathbf{z}^\pm}$, an upper bound of $\|\mathbf{z}^\pm\|^2$ is computed as

$$\|\kappa\hat{\boldsymbol{\sigma}}^{\mathrm{e}} \pm \frac{1}{\kappa}\hat{\boldsymbol{\sigma}}^{\mathrm{d,e}}\|_\sigma \geq \|\mathbf{z}^\pm\|. \tag{35}$$

As previously announced, expression (35) allows computing bounds for $L^{\mathcal{O}}(\hat{\mathbf{e}})$ without any use of the symmetrized error equations (30). In fact, the introduction of the symmetrized error equations is only a mathematical artifact that allows deriving an alternative bounding expression. The final bounds for $L^{\mathcal{O}}(\mathbf{u})$ are derived substituting expression (35) in equation (31):

$$\zeta_{\mathrm{U}} := L^{\mathcal{O}}(\hat{\mathbf{u}}) + \frac{1}{4}\|\kappa\hat{\boldsymbol{\sigma}}^{\mathrm{e}} + \frac{1}{\kappa}\hat{\boldsymbol{\sigma}}^{\mathrm{d,e}}\|_\sigma^2 - \hat{\alpha},$$
$$\zeta_{\mathrm{L}} := L^{\mathcal{O}}(\hat{\mathbf{u}}) - \frac{1}{4}\|\kappa\hat{\boldsymbol{\sigma}}^{\mathrm{e}} - \frac{1}{\kappa}\hat{\boldsymbol{\sigma}}^{\mathrm{d,e}}\|_\sigma^2 - \hat{\alpha},$$

where ζ_{U} and ζ_{L} are such that

$$\zeta_{\mathrm{L}} \leq L^{\mathcal{O}}(\mathbf{u}) \leq \zeta_{\mathrm{U}}. \tag{37}$$

Note that $\hat{\boldsymbol{\sigma}}^{\mathrm{e}}$ and $\hat{\boldsymbol{\sigma}}^{\mathrm{d,e}}$ are eventually computed using asymptotic techniques, for instance the flux-free strategies. In this case, the upper bound properties (37) hold only asymptotically, that is if the size of the reference mesh is *small enough*. In practice, due to the overestimation introduced in the subsequent approximations, the estimates obtained are upper bound of the error in all the examples. The parameter κ is determined such that it minimizes $\|\kappa\hat{\boldsymbol{\sigma}}^{\mathrm{e}} \pm \frac{1}{\kappa}\hat{\boldsymbol{\sigma}}^{\mathrm{d,e}}\|_{\sigma}^2$.

7 NUMERICAL EXAMPLE

The second numerical example illustrates the performance of the bounds in a full 2D problem. This example is inspired in one from [32]. It consists of a rectangular plate initially at rest which is loaded with two impulsive tractions, see figure 1. This action generates elastic waves propagating along the plate and reaching to the region of interest $\Omega^{\mathcal{O}}$. The quantity of interest is an average of velocities in this region during a time interval (selected such that the wave is noticeable in this region, see figure 2). This quantity is defined as

$$L^{\mathcal{O}}(\mathbf{w}) := \int_I \alpha(t) l^{\mathcal{O}}(\dot{\mathbf{w}}(t))\, \mathrm{d}t,$$

where

$$l^{\mathcal{O}}(\mathbf{w}) := (\mathbf{f}^{\mathcal{O}}, \mathbf{w}),$$

and

$$\mathbf{f}^{\mathcal{O}}(\mathbf{x}) := \begin{cases} \dfrac{-\mathbf{e}_2}{\mathrm{meas}(\Omega_{\mathcal{O}})} & \mathbf{x} \in \Omega_{\mathcal{O}} \\ \mathbf{0} & \text{else} \end{cases}.$$

Vector $\mathbf{e}_2$ is the unit vector in the y–axis and $\alpha(t)$ is defined in figure 1(c). All the parameters involved in the problem are specified in table 1.

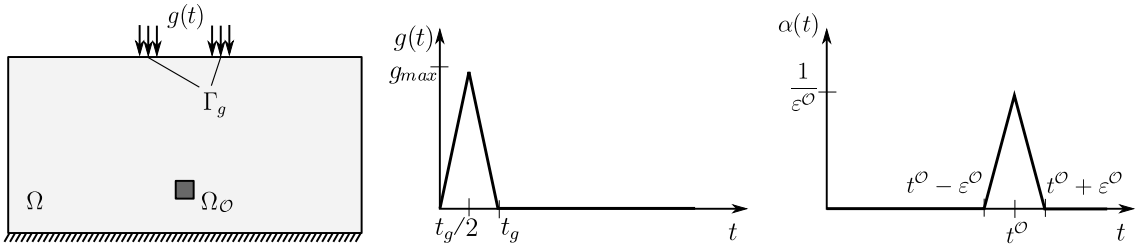

(a) Problem geometry (b) Time dependence of external load (c) Time dependence of the quantity of interest extractor

Figure 1: Example 2: Problem statement and quantity of interest.

The problem is solved with three different meshes with decreasing element size, see table 2. In all cases linear triangles are considered. The time step is chosen such that $\Delta t = 0.8H/c$. The reference mesh for the flux-free method is taken as $h := H/4$. The value of the *exact* solution $\mathbf{u}$ displayed in some figures and tables correspond to the reference solution obtained with the finer mesh (mesh 3) Other parameters related with the discretization are given in table 2.

Several snap shots of the numerical solution of the original and adjoint problems are shown in figures 3, 4 and 5 for the three values of the viscosity under consideration. The damping factors ξ associated with the values of the viscosity parameter, 10^{-4}s, 10^{-3}s and 10^{-2}s, are 0.0247%, 0.247% and 2.47% respectively. Note that for the original problem the elastic waves propagate forward in time, and backward in time for the adjoint.

Table 1: Example 2: Parametrization

Geometry			Material properties		
Ω	$(-0.5, 0.5) \times (0, 0.5)$	m^2	E	$8/3$	Pa
$\Omega_{\mathcal{O}}$	$(-0.025, 0.025) \times (0.1, 0.15)$	m^2	ν	$1/3$	
Γ_g	$[(0.075, 0.125) \cup (-0.075, -0.125)] \times (0.5)$	m	ρ	1	kg/m^3
T	0.25	s	τ	$\{10^{-4}, 10^{-3}, 10^{-2}\}$	s
			ξ	$\{0.0247, 0.247, 2.47\}$	%
External load			**Quantity of interest**		
g_{max}	30	Pa	$\varepsilon^{\mathcal{O}}$	0.01	s
t_g	0.005	s	$t^{\mathcal{O}}$	0.2170	s

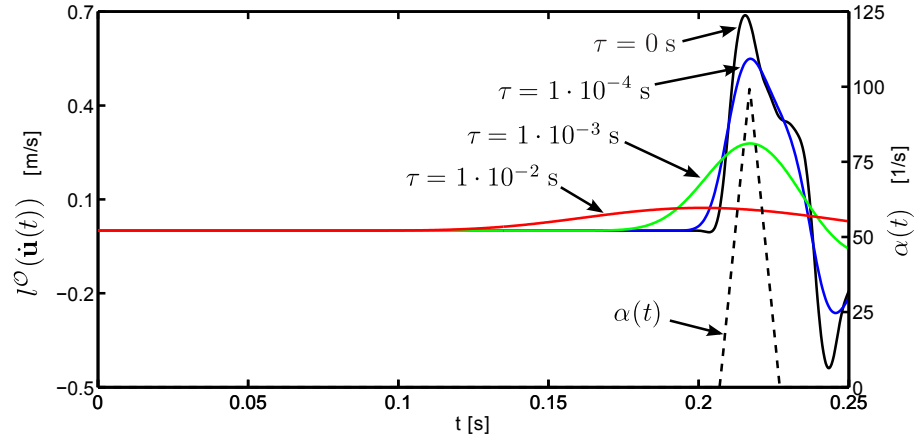

Figure 2: Example 2: Time evolution of the of the average $l^{\mathcal{O}}(\dot{\mathbf{u}}(t))$ for three values of the viscosity (left y-axis) and time evolution of the weighting function $\alpha(t)$ (right y-axis).

Table 2: Example 2: Space and time discretizations.

	D.O.F.	H [mm]	# elements	N
mesh 1	24000	0.16	23596	325
mesh 2	95190	0.08	94384	650
mesh 3	379146	0.04	377536	1300

Figure 6 shows the computed value $L^{\mathcal{O}}(\hat{\mathbf{u}})$ and the bounds obtained for the three values of the viscosity and decreasing element size. In addition, table 3 shows the effectivity of the computed bounds. Note that in this case the bounds are also sharper for higher values of τ and for smaller element sizes. In particular, for $\tau = 10^{-4}$s and $\tau = 10^{-3}$s the bounds are not sharp at all, even for mesh number 3, which can be considered an overkill mesh. Note that, in these two cases, the bounds do not allow identifying which is the sign of the quantity of interest. For $\tau = 10^{-2}$s the bounds are much sharper. The proposed bounds reduce in approximately 50%

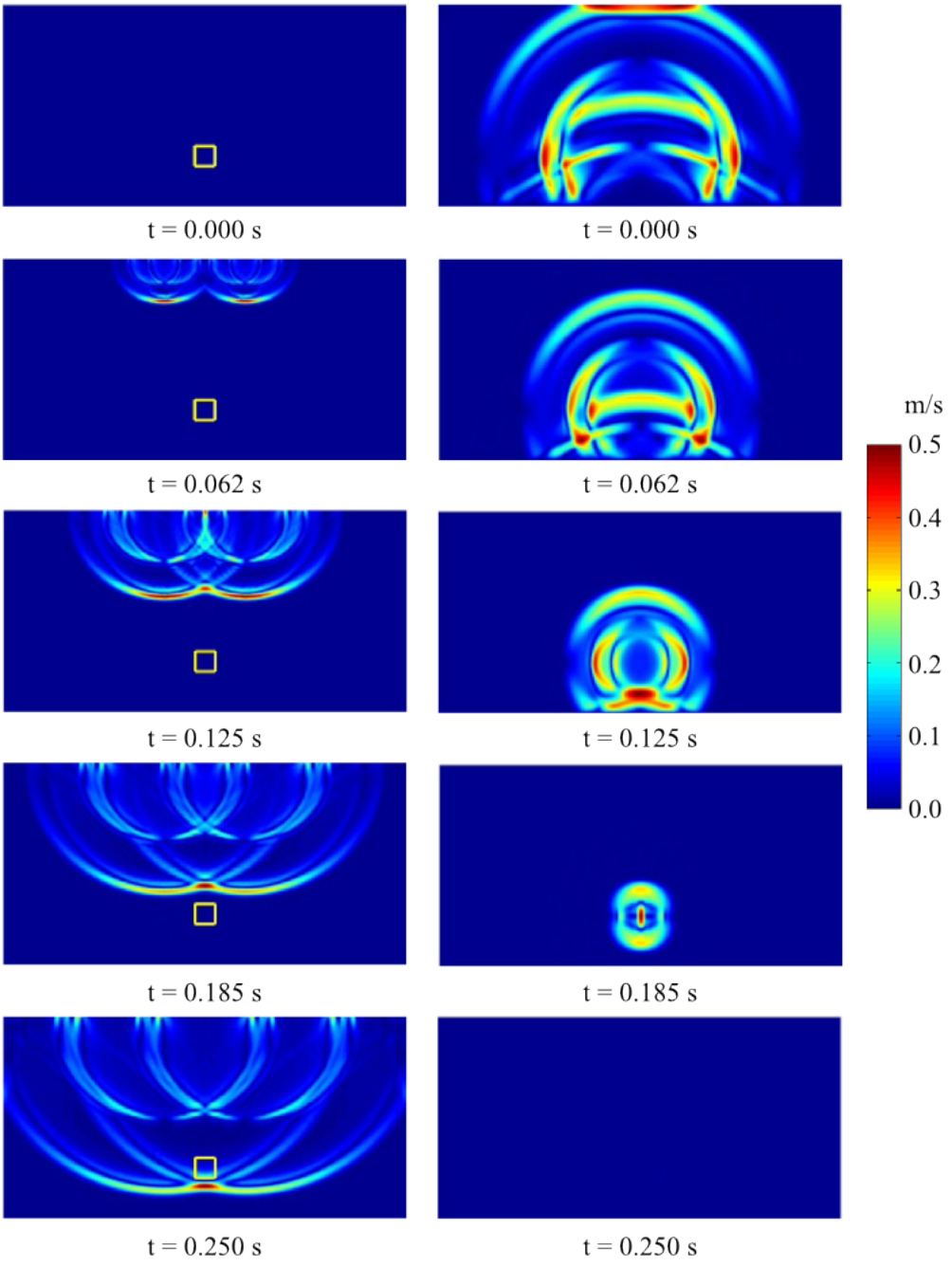

Figure 3: Example 2: Magnitude of the original (left) and adjoint (right) velocities for $\tau = 10^{-4}$ s ($\xi = 0.0247\%$).

the bound gap with respect to the ones based on the Cauchy-Schwarz inequality, in all cases. Note however that for the small values of the viscosity, $\tau = 10^{-4}$s and $\tau = 10^{-3}$s, this reduction is not sufficient to have bounds applicable in practical engineering examples.

8 CONCLUSIONS

- Bounds for linear functional outputs are derived for linear visco-elastodynamics. A new bounding expression is presented which improves the quality with respect to the previous approaches based on the Cauchy-Schwarz inequality. The proposed new approach is based on an alternative error representation, involving symmetrized error equations,

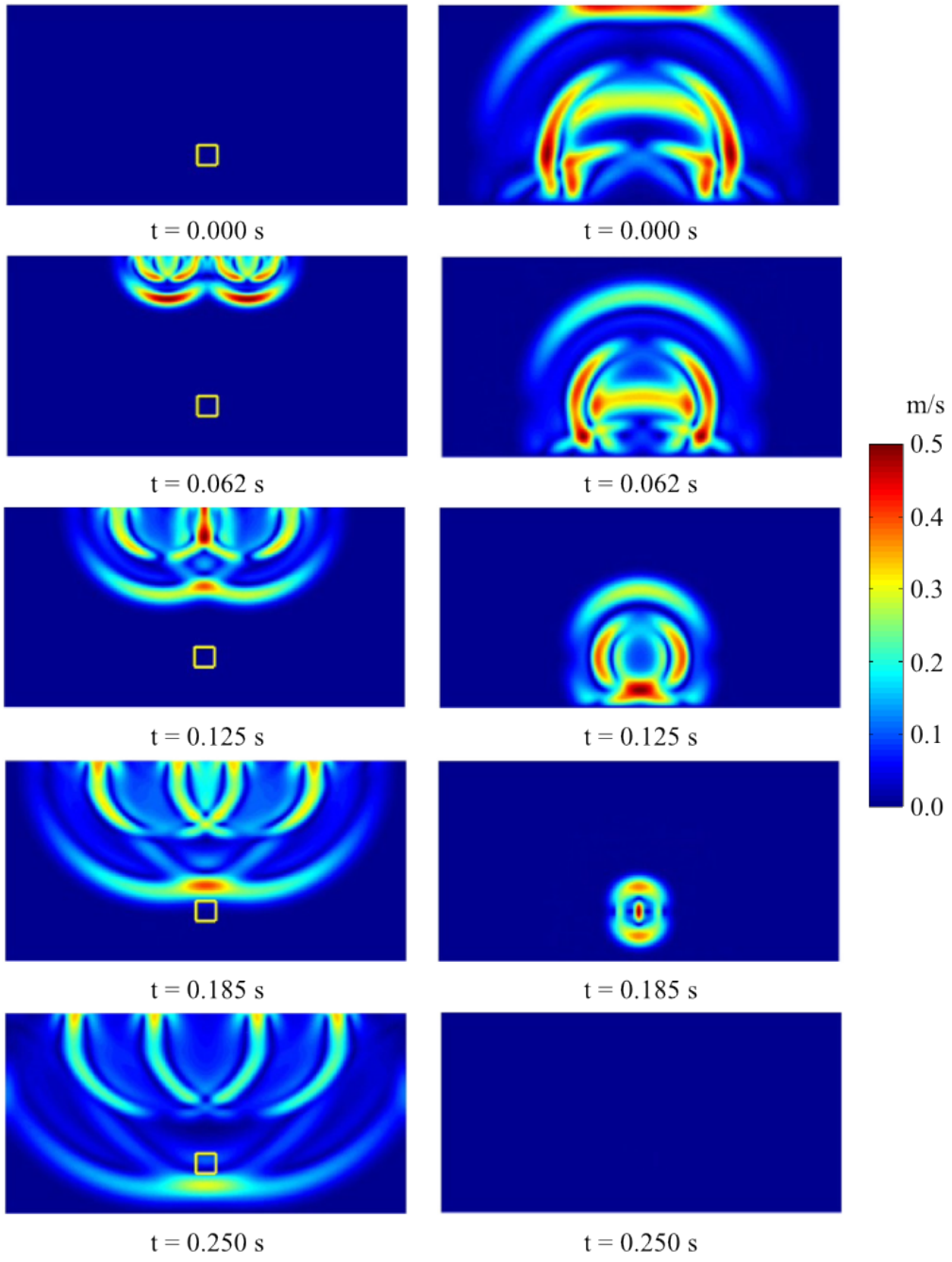

Figure 4: Example 2: Magnitude of the original (left) and adjoint (right) velocities for $\tau = 10^{-3}$ s ($\xi = 0.247\%$).

which is derived precluding the use of the Cauchy-Schwarz inequality.

- The key ingredient for the practical application of the method is the construction of admissible fields for both the original and adjoint problems. The proposed formulation is valid for any numerical method, provided that the numerical solution furnishes admissible fields (possibly after some post processing). Here, the K-admissible field is computed as a post process of the Newmark solution. On the other hand, the D-admissible field is computed with the asymptotic flux-free strategy. This method is based on a reference mesh and therefore, the proposed bounds hold when the element size of the reference mesh is fine enough. In practice, the numerical examples show that the computed values

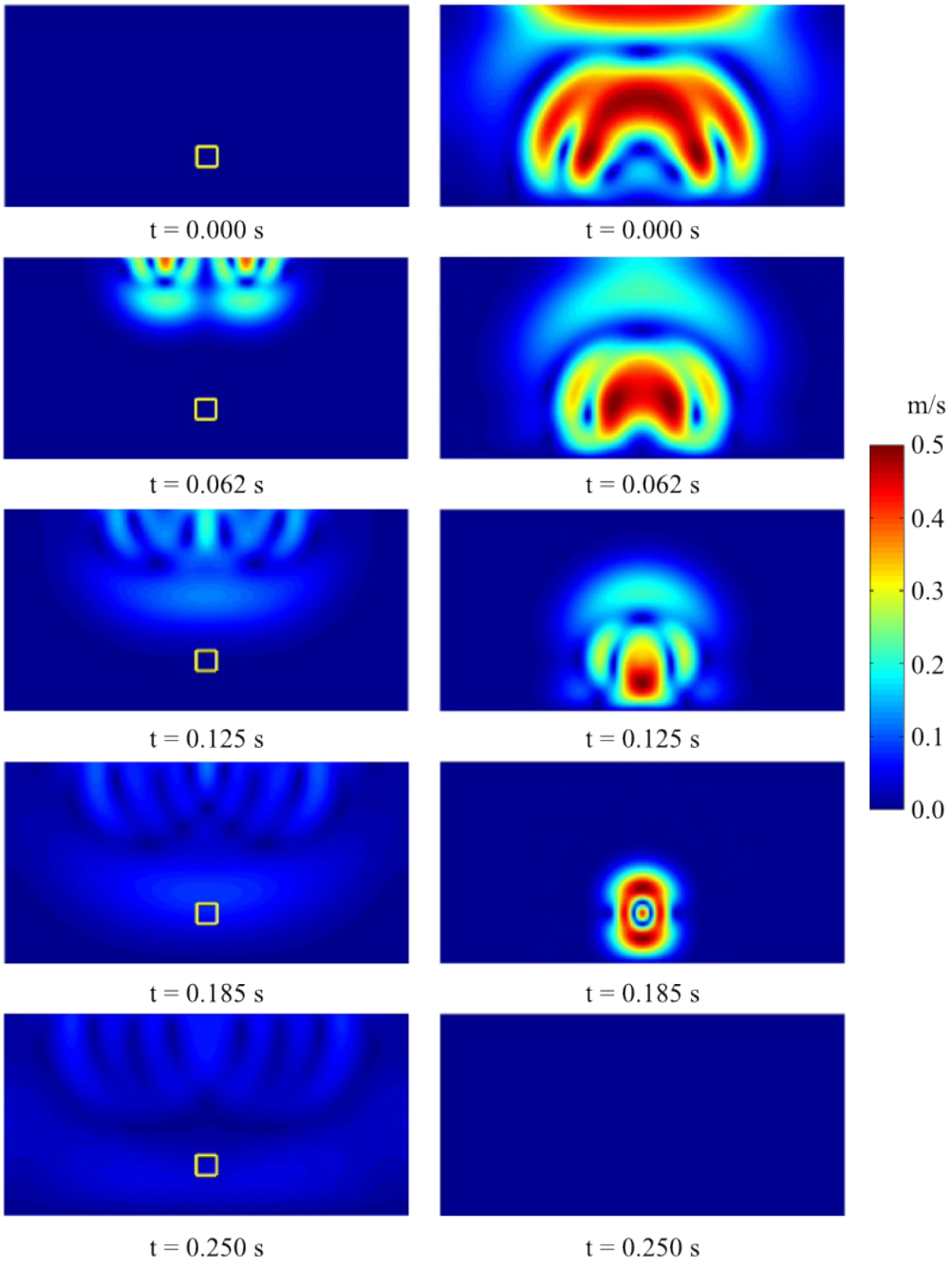

Figure 5: Example 2: Magnitude of the original (left) and adjoint (right) velocities for $\tau = 10^{-2}$ s $\xi = (2.47\%)$.

are indeed true bounds of the quantity of interest.

- All the developments in the paper require that the formulation includes a certain amount of viscosity. In the present case, the linear Kelvin-Voigt model is considered. The quality of the results obtained degenerate in the limit case of elasticity (zero or very small viscosity). In materials with small amounts of viscosity, the bounds obtained are pessimistic. The numerical tests reveal that when the meshes are refined the bound gap tends to be reduced and, correspondingly, the strategy provides sharp bounds for fine enough meshes. Nevertheless, in practice, for low viscosity, the meshes providing accurate bounds are not computationally affordable. Therefore, further research is needed to explore alternative

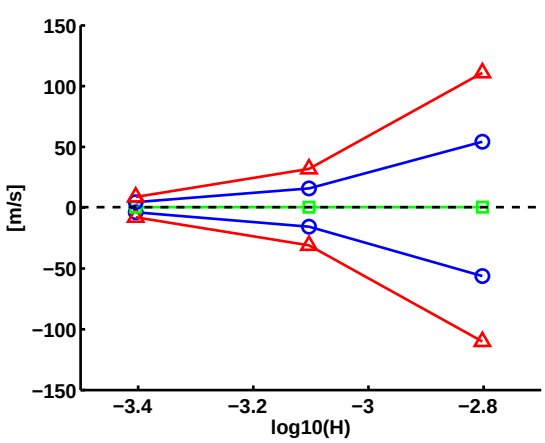

(a) $\tau = 1 \cdot 10^{-6}$ s ($\xi = 0.0247\%$)

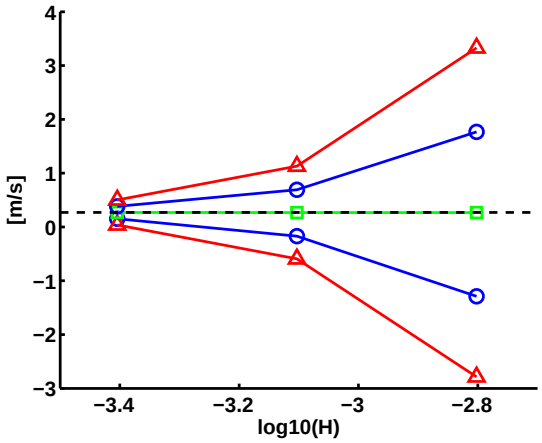

(b) $\tau = 1 \cdot 10^{-5}$ s ($\xi = 0.247\%$)

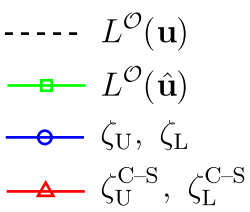

(c) Legend

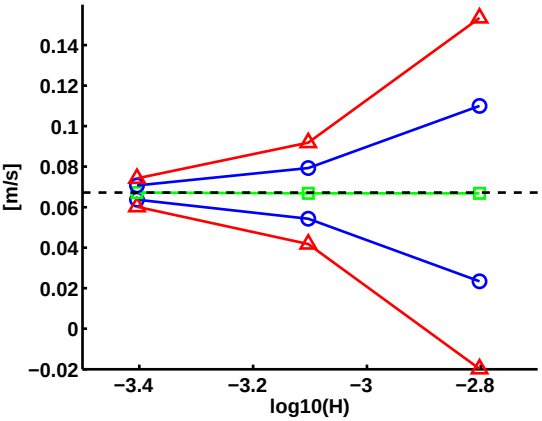

(d) $\tau = 1 \cdot 10^{-4}$ s ($\xi = 2.47\%$)

Figure 6: Example 2: Convergence of the computed bounds for different values of element size and viscosity.

Table 3: Example 2: Convergence of the computed bounds. Results in [m/s].

τ [s]	D.O.F.	$L^{\mathcal{O}}(\hat{\mathbf{u}})$	$L^{\mathcal{O}}(\mathbf{u})$	$\frac{\zeta_{\mathrm{U}}}{L^{\mathcal{O}}(\mathbf{u})}$	$\frac{\zeta_{\mathrm{L}}}{L^{\mathcal{O}}(\mathbf{u})}$	$\frac{\zeta_{\mathrm{U}}^{\mathrm{C\text{–}S}}}{L^{\mathcal{O}}(\mathbf{u})}$	$\frac{\zeta_{\mathrm{L}}^{\mathrm{C\text{–}S}}}{L^{\mathcal{O}}(\mathbf{u})}$
$1 \cdot 10^{-4}$	24000	0.4937	0.4960	110.0524	-113.8099	224.8397	-222.8850
	95190	0.4932	0.4960	32.1210	-31.5976	64.7088	-62.7284
	379146	0.4960	0.4960	9.2333	-7.6063	17.8371	-15.8420
$1 \cdot 10^{-3}$	24000	0.2681	0.2697	6.5943	-4.8098	12.4183	-10.3898
	95190	0.2681	0.2697	2.5800	-0.6352	4.2187	-2.2117
	379146	0.2697	0.2697	1.4224	0.5637	1.8595	0.1422
$1 \cdot 10^{-2}$	24000	0.0668	0.0672	1.6457	0.3498	2.2953	-0.2967
	95190	0.0668	0.0672	1.1867	0.8121	1.3745	0.6252
	379146	0.0672	0.0672	1.0520	0.9477	1.1043	0.8956

pertinent bounds for nearly elastic problems.

ACKNOWLEDGEMENT

Supported by the Universitat Politècnica de Catalunya (UPC-BarcelonaTech), Grant UPC-FPU-2009. Partially supported by Ministerio de Educacin y Ciencia, Grant DPI2011-27778-C02-02. The support of the Col·legi d'Enginyers de Camins, Canals i Ports (Catalunya) is also greatfuly acknowledged.

REFERENCES

[1] I Babuŝka and WC Rheinboldt. Error estimates for adaptive finite element computations. *SIAM J. Numer. Anal.*, 18:736–754, 1978.

[2] P Ladevèze and D Leguillon. Error estimate procedure in the finite element method. *SIAM J. on Numerical Analysis*, 20:485–509, 1983.

[3] OC Zienkiewicz and JZ Zhu. A simple error estimator and adaptative procedure for practical engineering analysis. *Int. J. Numer. Meth. Engrg.*, 24:337–357, 1987.

[4] M Paraschivoiu, J Peraire, and AT Patera. A posteriori finite element bounds for linear-functional outputs of elliptic partial differential equations. *Comput. Methods Appl. Mech. Engrg.*, 150:289–321, 1997.

[5] N Parés, J Bonet, A Huerta, and J Peraire. The computation of bounds for linear-functional outputs of weak solutions to the two-dimensional elasicity equations. *Comput. Methods Appl. Mech. Engrg.*, 195:406–429, 2006.

[6] F Cirak and E Ramm. A posteriori error estimation and adaptivity for linear elasticity using the reciprocal theorem. *Comput. Methods Appl. Mech. Engrg.*, 156:351–362, 1998.

[7] S Prudhomme and JT Oden. On goal-oriented error estimation for elliptic problems: application to the control of pointwise errors. *Comput. Methods Appl. Mech. Engrg.*, 176:313–331, 1999.

[8] D Aubry, D Lucas, and B Tie. Adaptive strategy for transient/coupled problems. Applications to thermoelasticity and elastodynamics. *Comput. Methods Appl. Mech. Engrg.*, 176:41–50, 1999.

[9] X Li and NE Wiberg. Implementation and adaptivity of a space-time finite element method for structural dynamics. *Comput. Methods Appl. Mech. Engrg.*, 156:211–229, 1998.

[10] NE Wiberg and X Li. Adaptive finite element procedures for linear and non-linear dynamics. *Int. J. Numer. Meth. Engrg.*, 46:178–1802, 1999.

[11] L Chamoin and P Ladevèze. A non-intrusive method for the calculation of strict and efficient bounds of calculated outputs of interest in linear viscoelasticity problems. *Comput. Methods Appl. Mech. Engrg.*, 197:994–1014, 2008.

[12] JP Combe, P Ladevèze, and JP Pelle. Discretization error estimator for transcient dynamic simulations. *Advances in Engrg. Software*, 33:553–563, 2002.

[13] JP Combe, P Ladevèze, and JP Pelle. Constitutive relation error estimator for transient finite element analysis. *Comput. Methods Appl. Mech. Engrg.*, 176:165–185, 1999.

[14] P Ladevèze and JP Pelle. Estimation of discretization errors in dynamics. *Computers and Structures*, 81:1133–1148, 2003.

[15] A Schleupen and E Ramm. Local and global error estimations in linear structural dynamics. *Computers and structures*, 76:741–756, 2000.

[16] D Fuentes, D Littlefiel, JT dOden, and S Prudhomme. Extensions of goal-oriented error estimation methods to simulation of highly-nonlinear response of shock-loaded elastomer-reinforced structures. *Comput. Methods Appl. Mech. Engrg.*, 195:4659–4680, 2006.

[17] P Ladevèze and J Waeytens. Model verification in dynamics trough strict upper bounds. *Comput. Methods Appl. Mech. Engrg.*, 198:1775–1784, 2009.

[18] J Waeytens. *Contrôle des calculs en dynamique: bornes strictes et pertinents sur une quantié d'intérêt*. PhD thesis, LMT-Cachan, 2010.

[19] P Ladevèze. Strict upper error bounds for computed outputs of interest in computational structural mechanics. *Computational Mechanics*, 42:271–286, 2008.

[20] J Waeytens, L Chamoin, and P Ladevèze. Guaranteed error bounds on pointwise quantities of interest for transient viscodynamics problems. *Computational Mechanics*, 49:291–307, 2012.

[21] N Parés, P Díez, and A Huerta. Bounds of functional outputs for parabolic problems. Part I: Exact bounds of the discontinuous galerkin time discretization. *Comput. Methods Appl. Mech. Engrg.*, 197:1641–1660, 2008.

[22] N Parés, P Díez, and A Huerta. A subdomain-based flux-free a posteriori error estimators. *Comput. Methods Appl. Mech. Engrg.*, 195:297–323, 2006.

[23] NM Newmark. A method of computation for structural dynamics. *J. of Engineering Mechanics*, 85:67–94, 1959.

[24] JR Hughes and M Hulbert. Space-time finite element methods for elastodynamics: Formulations and error estimates. *Comput. Methods Appl. Mech. Engrg.*, 66:339–363, 1988.

[25] M Hulbert and JR Hughes. Space-time finite element methods for second-order hypeerbolic equations. *Comput. Methods Appl. Mech. Engrg.*, 84:327–348, 1990.

[26] P Ladevèze and JP Pelle. *La maîtrise du calcul en mécanique linéaire et non linéaire*. Lavoisier, 2001.

[27] M Ainsworth and JT Oden. *A posteriori error estimation in Finite element analysis*. John Wiley & Sons Ltd., 2000.

[28] R Cottereau, P Díez, and A Huerta. Strict error bounds for linear solid mechanics problems using a subdomain-based flux-free method. *Comput. Mech.*, 44:533–547, 2009.

[29] J P Moitinho de Almeida and O J B Almeida Pereira. Upper bounds of the error in local quantities using equilibrated and compatible finite element solutions for linear elastic problems. *Comput. Methods Appl. Mech. Engrg.*, 195:279–296, 2006.

[30] O J B Almeida Pereira and J P Moitinho de Almeida. Dual adaptive finite element refinement for multiple local quantities in linear elastostatics. *Int. J. Numer. Meth. Engrg.*, 83:347–365, 2010.

[31] JT Oden and S Prudhomme. Goal-oriented error estimation and adaptivity for the finite element method. *Computers and Math. with Appl.*, 41:735–765, 2001.

[32] NC Nguyen, J Peraire, and B Cockburn. High-order implicit hybridizable discontinuous Galerkin methods for acoustics and elastodynamics. *Journal of Computational Physics*, 230:3695–3718, 2011.